Alexandria Engineering Journal (2022) 61, 17–27

HOSTED BY

ELSEVIER

Alexandria University

Alexandria Engineering Journal

www.elsevier.com/locate/aej
www.sciencedirect.com

Unsteady flow of fractional Burgers' fluid in a rotating annulus region with power law kernel

Maria Javaid [a], Madeeha Tahir [b], Muhammad Imran [a,*], Dumitru Baleanu [c,d,e], Ali Akgül [f,*], Muhammad Asjad Imran [g]

[a] Department of Mathematics, Government College University Faisalabad, 38000, Pakistan
[b] Department of Mathematics, Government College Women University Faisalabad, 38000, Pakistan
[c] Department of Mathematics, Cankaya University, 06530 Balgat, Ankara, Turkey
[d] Institute of Space Sciences, R76900 Magurele-Bucharest, Romania
[e] Department of Medical Research, China Medical University, Taichung 40402, Taiwan
[f] Department of Mathematics, Art and Science Faculty, Siirt University, 56100 Siirt, Turkey
[g] Department of Mathematics, University of Management and Technology Lahore, Lahore 54770, Pakistan

Received 18 November 2020; revised 8 March 2021; accepted 24 April 2021
Available online 2 July 2021

KEYWORDS

Fractional Burgers' fluid;
Annulus;
Integral transform;
Modified Bessel equation;
Gaver-Stehfest's algorithm

MATHEMATICS SUBJECT CLASSIFICATION (2010)

76A05

Abstract Keeping in view of the complex fluid mechanics in bio-medicine and engineering, the Burgers' fluid with a fractional derivatives model analyzed through a rotating annulus. The governing partial differential equation solved for velocity field and shear stress by using integral transformation method and using Bessel equations. The transformed equation inverted numerically by using Gaver-Stehfest's algorithm. The approximate analytical solution for rotational velocity, and shear stress are presented. The influence of various parameters like fractional parameters, relaxation and retardation time parameters material constants, time and viscosity parameters are drawn numerically. It is found that the relaxation time and time helps the flow pattern, on the other hand other material constants resist the fluid rotation. Fractional parameters effect on fluid flow is opposite to each other. Finally, to check the validity of the solution there are comparisons for velocity field and shear stress for obtained results with an other numerical algorithm named Tzou's algorithm.

1. Introduction

Fluids play an important role in every field of life. Therefore it is necessary to study fluids, especially fluids in motion (fluid dynamics). In the present era it is very important to study non-Newtonian fluids, may be in translational and rotational motion, because of their cosmic application in industrial area.

* Corresponding authors.
E-mail addresses: drmimrachaudhry@gcuf.edu.pk (M. Imran), aliakgul00727@gmail.com (A. Akgül).

Peer review under responsibility of Faculty of Engineering, Alexandria University.

https://doi.org/10.1016/j.aej.2021.04.106
1110-0168 © 2021 THE AUTHORS. Published by Elsevier BV on behalf of Faculty of Engineering, Alexandria University.

In past few decades non-Newtonian fluids with ordinary derivatives are interesting point of research for the researchers. Ting [1] discussed the unsteady flows of a second grade through a bounded boundary in (1963). Waters and King [2] (1971) studied the unsteady flow of an elastico-viscous liquid in a straight pipe of circular cross section in the presence of constant pressure gradient and found that velocity of the fluid depends on the elastic parameters. Fetecău and Fetecău [3] (1985) discussed the uniqueness of some helical flows of a second grade fluid, between two infinite circular cylinders. He studied the problem by considering time dependent shear stress on cylinders and impact of physical parameters on the velocity and shear stress. Rahaman and Ramkissoon [4] (1995) examined in detail the basic unsteady pipe flows to investigate the new physical phenomena. He considered the viscoelastic upper-convected Maxwell fluid as non-Newtonian model in pipes of uniform circular cross-section and studied the following three cases to give the results in close form by using Bessel equations: (a) when the pressure gradient varies exponentially with time; (b) when the pressure gradient is pulsating; (c) a starting flow under a constant pressure gradient. Wood [5] (2001) studied start-up helical flows for Oldroyd-B and upper-convected Maxwell fluids in straight pipes of circular and annular cross-section. Hayat et al. [6] (2001) obtained exact solutions for the following five problems of an Oldroyd-B fluid by applying integral transforms to governing partial differential equations (i) Stokes problem (ii) modified Stokes problem (iii) the time-periodic Poiseuille flow due to an oscillating pressure gradient (iv) the non-periodic flows between two boundaries, and (v) symmetric flow with an arbitrary initial velocity. Fetecau [7] (2004) obtained analytical solutions for non-Newtonian fluid flows in pipe-like domains. Sajid et al. [8] (2008) performed an analysis for the boundary-layer flow of a viscous fluid over a nonlinear axisymmetric stretching sheet by using Homotopy Analysis Methods with the help of similarity transformation method. Fetecau et al. [9] (2010) obtained exact solutions corresponding to the unsteady helical flow of an Oldroyd-B fluid due to an infinite circular cylinder subject to torsional and longitudinal time-dependent shear stresses by using Hankel transforms and found the steady state solutions for the fluid model.

Recently, fractional derivatives approach proved itself a useful tool for dealing the fluid which have both viscous and elastic properties. It comes under the field of applied mathematics which involve the derivatives and integral of arbitrary orders. During the last decade fractional calculus has been applied to almost every field of science, engineering and mathematics [10,11]. Due to its vast advantageous in the field of waves propagation [12], thermodynamics [13], bio-engineering [14] and bio-rheology [15] because of power-law responses from many tissue-like materials [16,17]. A well known example of such power-law is elastic tissues of the aorta [18,19]. Jiméneza et al. [20] (2002) studied stress relaxation in samples of polymers PMMA and PTFE (Methylmethacrylate and Polytetrafluorethylene), pointed out that there exists not only one time of relaxation as the classic Maxwell model predicts but two distributions of relaxation time. The fractional derivative approach in the studying fluid dynamics has the benefit that it can affords the possibilities of complex constitutive equations for viscoelastic materials with only few experimentally determined parameters.

The age in which we live can rightly be called the age of science and technology. It is time consuming procedure to solve the equation with higher order derivatives analytically. One can use some software for it. In the late 1960s the Gaver-Stehfest algorithm for numerical inversion of Laplace transform was constructed. Due to its good performance it become popular almost ever field of science like mathematics, physics, sociology, economics and chemistry. In fluid dynamics for calculation mostly integral transform is used as a basic tool. Villinger (1985) has investigated the inhomogeneous one dimensional heat diffusion equation [21]. Akgül et al. [22] (2015) studied numerical solutions of fractional differential equations of Lane-Emden type by an accurate technique. In (2017) a numerical investigation on Burgers equation by MOL-GPS method obtained by Hashemi et al. [23]. Raza [24] has investigated the unsteady rotational flow of a second grade fluid in details by using Caputo derivative operator. Wang et al. [25] (2019) have studied Oldroyd-B fluid through rotating annulus by utilizing Laplace transforms and modified Bessel equation, for inverse Laplace transform numerical procedure (Gaver Stehfest algorithm) was used. Qureshi and Yusuf [11] studied, an epidemiological model (MSEIR) of varicella disease outbreak, also called the chickenpox, among school children in the Shenzhen city of China in 2015 was proposed under three most commonly used approaches, such as the Caputo, Caputo-Fabrizio and the Atangana-Baleanu-Caputo operators. Numerical simulations are carried out for the analysis of the model. Qureshi et al. [26] used, a newly devised integral transform called the Mohand transform to find the exact solutions of fractional-order ordinary differential equations under the Caputo type operator.

In this article the results concerning the unsteady flow of fractional Burgers' fluid in a rotating annulus, in which both the cylinders apply shear stress to the fluid, are obtained. Both cylinder and fluid taken at rest initially, after some specific time both cylinder force to rotate by some external force. The expressions for the velocity and shear stress are given in Laplace transform domain with the aid of modified Bessel equations which fulfill all the imposed conditions. Inversion of the Laplace transformation done numerically by using MATCAD software. At the end, influence of various parameters like fractional parameters, relaxation and retardation time parameters material constants, time and viscosity parameters are drawn numerically. Finally, to check the validity of the solution there are comparisons for velocity field and shear stress for obtained results with an other numerical algorithm named Tzou's algorithm.

1.1. Methodology

In (2006) Debnath & Bhatta in their book *Integral Transforms and their Applications* [27] define infinite and finite Laplace transform. The Laplace transform of $g(t)$ in $0 < t < \infty$ is defined as,

$$G(s) = \mathscr{L}\{g(t)\} = \bar{g}(s) = \int_0^\infty e^{-st} g(t)dt; \quad \mathrm{Re}\, s > 0, \tag{1}$$

where, e^{-st} is kernel of the transform and s is transformed variable. The finite Laplace transform of a continuous function $f(t)$ in $(0, T)$ is defined as

$$G(s) = L\{g(t)\} = \bar{g}(s) = \int_0^T e^{-st} g(t)dt, \tag{2}$$

where s is a real or complex number and T is a finite number that may be positive or negative so that Eq. (2) can be defined in any interval $(-T_1, T_2)$.

For solving differential equation (DE) by numerical methods, numerical algorithms are used. In 1960s, "the Gaver-Stehfest" defined an algorithm useful to find the inverse Laplace transform of (simple and complicated expressions equally) the expressions numerically by sequence of functions [28].

$$g(t) = \frac{\ln 2}{t} \sum_{k=1}^{2p} d_k \bar{u}\left(k \frac{\ln(2)}{t}\right), \tag{3}$$

where p is a positive integer and

$$d_k = (-1)^{k+p} \sum_{s=\left[\frac{k+1}{2}\right]}^{\min(k,p)} \frac{i^p (2p)!}{(p-s)!s!(s-1)!(k-s)!(2s-k)!}.$$

Tzou's give another algorithm to find the inverse Laplace transform of complicated expressions numerically by sequence of functions [29]

$$f_n(x) = \frac{\exp 4.7}{t}\left[0.5F\left(\frac{4.7}{t} + \Re\left(\sum_{l=1}^{L_1} (-1)^k F\left(\frac{4.7 + i\pi}{t}\right)\right)\right)\right], \tag{4}$$

where $\Re(\cdot)$ is the real part, i is the imaginary unit and $L_1 \gg 1$ is a natural number.

2. Governing equations

Let us assume a fractional Burgers' fluid which is incomprehensible in an annulus. At time $t > 0$, both cylinders having radii R_1 and $R_2(> R_1)$ start rotating along their axis. The constitutive equation for Burgers' fluid are [30–32]

$$\mathbf{T} = -p\mathbf{I} + \mathbf{S}\ ;\ \left(\mathbf{1} + \lambda \frac{\delta}{\delta \mathbf{t}} + \lambda_1 \frac{\delta^2}{\delta \mathbf{t}^2}\right)\mathbf{S} = \mu\left(\mathbf{1} + \lambda_r \frac{\delta}{\delta \mathbf{t}}\right)\mathbf{A}, \tag{5}$$

$$\frac{\delta \mathbf{S}}{\delta t} = \left(\frac{d}{dt} - \mathbf{L} - \mathbf{L}^{\mathbf{T}}\right)\mathbf{S}.$$

For the considered problem velocity field $\mathbf{V}$ and extra-stress tensor $\mathbf{S}$ have the following form,

$$\mathbf{V} = \mathbf{V}(r,t) = v_\theta(r,t)\mathbf{e}_\theta;\ \ \mathbf{S} = \mathbf{S}(r,t). \tag{6}$$

For such flows equation of continuity is automatically satisfied.

At $t = 0$,

$$\mathbf{V}(r,0) = \mathbf{0};\quad \mathbf{S}(r,0) = \mathbf{0}. \tag{7}$$

The governing equations [30,32] are presented as:

$$\left(1 + \lambda \frac{\partial}{\partial t} + \lambda_1 \frac{\partial^2}{\partial t^2}\right)\tau(r,t) = \mu\left(1 + \lambda_r \frac{\partial}{\partial t}\right)\left(\frac{\partial}{\partial r} - \frac{1}{r}\right)v_\theta(r,t), \tag{8}$$

where $\tau(r,t) = S_{r\theta}(r,t)$ is the shear stress.

$$\left(1 + \lambda \frac{\partial}{\partial t} + \lambda_1 \frac{\partial^2}{\partial t^2}\right)\frac{\partial v_\theta(r,t)}{\partial t} = \nu\left(1 + \lambda_r \frac{\partial}{\partial t}\right)\left(\frac{\partial^2}{\partial r^2} + \frac{1}{r}\frac{\partial}{\partial r} - \frac{1}{r^2}\right)v_\theta(r,t). \tag{9}$$

The governing equations are obtained as [33,34]:

$$\left(1 + \lambda D_t^\alpha + \lambda_1 D_t^{2\alpha}\right)\tau(r,t) = \mu\left(1 + \lambda_r D_t^\beta\right)\left(\frac{\partial}{\partial r} - \frac{1}{r}\right)v_\theta(r,t), \tag{10}$$

$$\left(1 + \lambda D_t^\alpha + \lambda_1 D_t^{2\alpha}\right)\frac{\partial v_z(r,t)}{\partial t} = \nu\left(1 + \lambda_r D_t^\beta\right)\left(\frac{\partial^2}{\partial r^2} + \frac{1}{r}\frac{\partial}{\partial r} - \frac{1}{r^2}\right)v_\theta(r,t), \tag{11}$$

where the Riemann-Liouville fractional differential operator D_t^α is defined by [35,36]

$$\mathrm{D}_t^\beta f(t) = \begin{cases} \frac{1}{|(1-\beta)} \frac{d}{dt} \int_0^t \frac{f(\tau)}{(t-\tau)^\beta} d\tau, & 0 \leqslant \beta < 1; \\ \frac{d}{dt} f(t), & \beta = 1. \end{cases} \tag{12}$$

3. The analytic solutions

Both cylinder and fluid taken at rest initially, after some specific time both cylinder force to rotate by some external force around their common axis. Due to the shear stress, the fluid is gradually rotate, its velocity being of the form Eq. (6). The governing equations are given by Eqs. (10), (11) while the relevant initial and boundary conditions are

$$v_\theta(r,0) = \frac{\partial v_\theta(r,0)}{\partial r} = 0;\ r \in [R_1, R_2], \tag{13}$$

$$v_\theta(R_1,t) = R_1\Omega_1 t;\ v_\theta(R_2,t) = R_2\Omega_2 t,\ t \geqslant 0. \tag{14}$$

3.1. Velocity field

Using Laplace transform Eq. (2) on Eqs. (11) and (14),

$$\left(q + \lambda q^{\alpha+1} + \lambda_1 q^{2\alpha+1}\right)\bar{v}_\theta(r,q) = \nu\left(1 + \lambda_r q^\beta\right)\left(\frac{\partial^2}{\partial r^2} + \frac{1}{r}\frac{\partial}{\partial r} - \frac{1}{r^2}\right)\bar{v}_\theta(r,q), \tag{15}$$

$$\bar{v}_\theta(R_1,q) = \frac{R_1\Omega_1}{q^2} = X(q);\ \bar{v}_\theta(R_2,q) = \frac{R_2\Omega_2}{q^2} = Y(q), \tag{16}$$

where $\overline{v_\theta}(r,q)$ is the Laplace transform of $v_\theta(r,t)$.

Eq. (15) can be written as,

$$\begin{aligned} &\frac{\partial^2 \bar{v}_\theta(r,q)}{\partial r^2} + \frac{1}{r}\frac{\partial \bar{v}_\theta(r,q)}{\partial r} - \frac{\bar{v}_\theta(r,q)}{r^2} \\ &\quad + \lambda_r q^\beta\left(\frac{\partial^2 \bar{v}_\theta(r,q)}{\partial r^2} + \frac{1}{r}\frac{\partial \bar{v}_\theta(r,q)}{\partial r} - \frac{\bar{v}_\theta(r,q)}{r^2}\right) \\ &\quad - \left(\frac{q + \lambda q^{\alpha+1} + \lambda_1 q^{2\alpha+1}}{\nu}\right)\bar{v}_\theta(r,q) = 0, \end{aligned} \tag{17}$$

$$\begin{aligned} &[1 + A(q)]\frac{\partial^2 \bar{v}_\theta(r,q)}{\partial r^2} + [1 + A(q)]\frac{1}{r}\frac{\partial \bar{v}_\theta(r,q)}{\partial r} \\ &- [1 + A(q)]\frac{\bar{v}_\theta(r,q)}{r^2} - B(q)\bar{v}_\theta(r,q) = 0, \end{aligned} \tag{18}$$

where

$$\lambda_r q^\beta = A(q) \quad \textit{and} \quad \frac{q + \lambda q^{\alpha+1} + \lambda_1 q^{2\alpha+1}}{\nu} = B(q). \tag{19}$$

Utilizing the $z = r\sqrt{\frac{B}{1+AB}} = rD$ in Eq. (18) gives:

$$z^2\frac{\partial^2\bar{v}_\theta}{\partial z^2}+z\frac{\partial\bar{v}_\theta}{\partial z}-\left(z^2-1\right)\bar{v}_\theta=0. \quad (20)$$

We obtain the general solution as [37]:

$$\bar{v}_\theta(z,q)=C_1I_1(z)+C_2K_1(z), \quad (21)$$

Where C_1 and C_2 are constants and I_1, K_1 modified Bessel functions.

Solve Eqs. (16) and (21) we obtain:

$$C_1=\frac{X(q)}{I_1(R_1D)}-\frac{K_1(R_1D)}{K_1(R_2D)I_1(R_1D)-K_1(R_1D)I_1(R_2D)}\left(Y(q)-X(q)\frac{I_1(R_2D)}{I_1(R_1D)}\right),$$

$$C_2=\frac{I_1(R_1D)}{K_1(R_2D)I_1(R_1D)-K_1(R_1D)I_1(R_2D)}\left(Y(q)-X(q)\frac{I_1(R_2D)}{I_1(R_1D)}\right).$$

Then, we take the values of C_1 and C_2 in Eq. (21) and we reach:

$$\bar{v}_\theta(r,q)=\left[\frac{X(q)}{I_1(R_1D)}-\frac{K_1(R_1D)}{K_1(R_2D)I_1(R_1D)-K_1(R_1D)I_1(R_2D)}\left(Y(q)-X(q)\frac{I_1(R_2D)}{I_1(R_1D)}\right)\right]I_1(rD)$$

$$+\left[\frac{I_1(R_1D)}{K_1(R_2D)I_1(R_1D)-K_1(R_1D)I_1(R_2D)}\left(Y(q)-X(q)\frac{I_1(R_2D)}{I_1(R_1D)}\right)\right]K_1(rD). \quad (22)$$

Eq. (22) is a complex Bessel functions. For solution, it is very difficult to solve traditionally.

3.2. Shear stress

In this section we will find shear stress from Eq. (10) with the help of Laplace transform

$$\left(1+\lambda q^\alpha+\lambda_1q^{2\alpha}\right)\bar{\tau}(r,q)=\mu\left(1+\lambda_rq^\beta\right)\left(\frac{\partial}{\partial r}-\frac{1}{r}\right)\overline{v_\theta}(r,q), \quad (23)$$

$$\bar{\tau}(r,q)=\mu\left(\frac{1+\lambda_rq^\beta}{1+\lambda q^\alpha+\lambda_1q^{2\alpha}}\right)\left(\frac{\partial\overline{v_\theta}(r,q)}{\partial r}-\frac{\overline{v_\theta}(r,q)}{r}\right), \quad (24)$$

let

$$\mu\left(\frac{1+\lambda_rq^\beta}{1+\lambda q^\alpha+\lambda_1q^{2\alpha}}\right)=\kappa.$$

$$\bar{\tau}(r,q)=\kappa\left(\frac{\partial\overline{v_\theta}(r,q)}{\partial r}-\frac{\overline{v_\theta}(r,q)}{r}\right), \quad (25)$$

Since, in (1962) Luke in his book *Integrals of Bessel Functions* explained [38]

$$\frac{\partial I_p}{\partial z}=I_{p+1}(z)-\frac{pI_p(z)}{z}.$$

$$\frac{\partial K_p}{\partial z}=-K_{p+1}(z)-\frac{pK_p(z)}{z}.$$

where, I_p and K_p are the modified Bessel functions of order p. Now using equation Eq. (22)

$$\frac{\partial\overline{v_\theta}(r,q)}{\partial r}-\frac{\overline{v_\theta}(r,q)}{r}=\left[\left[\frac{X(q)}{I_1(R_1D)}-\frac{K_1(R_1D)}{K_1(R_2D)I_1(R_1D)-K_1(R_1D)I_1(R_2D)}\times\left(Y(q)-X(q)\frac{I_1(R_2D)}{I_1(R_1D)}\right)\right]\left[DI_0(rD)-2\frac{I_1(rD)}{r}\right]\right.$$

$$\left.-\left[\frac{I_1(R_1D)}{K_1(R_2D)I_1(R_1D)-K_1(R_1D)I_1(R_2D)}\times\left(Y(q)-X(q)\frac{I_1(R_2D)}{I_1(R_1D)}\right)\right]\left[DK_0(rD)+2\frac{K_1(rD)}{r}\right]\right].$$

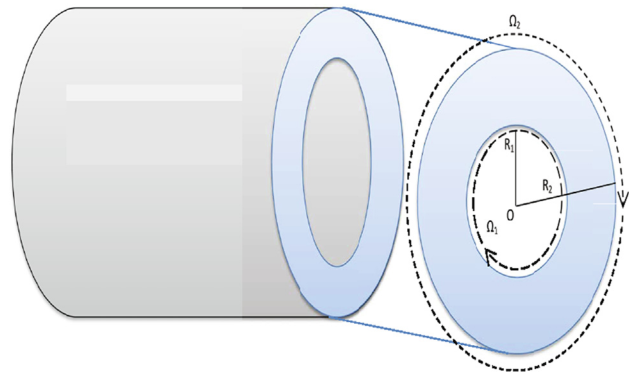

Fig. 1 Problem's Geometry.

Table 1 $v_\theta(r,t)$, Eq. (22) for $R_1=0.7$, $R_2=1$, $\Omega_1=0.5$, $\Omega_1=-0.5$, $\lambda=2$, $\lambda_1=1$, $\lambda_r=1$, $v=0.02$, $\alpha=0.1$, $\beta=1$, distinctness in time.

r	$v_\theta(r,t)$ t = 1	$v_\theta(r,t)$ t = 2	$v_\theta(r,t)$ t = 3
0.7	0.350077167	0.701659184	1.050474295
0.72	0.264881688	0.546549575	0.833351955
0.74	0.197553327	0.415995909	0.641711918
0.76	0.140877696	0.302495996	0.468979292
0.78	0.092327115	0.203700968	0.316131144
0.8	0.050637898	0.111262634	0.168248814
0.82	0.013237053	0.024862746	0.029207354
0.84	−0.024301236	−0.05670639	−0.105393833
0.86	−0.061483619	−0.140850945	−0.238743968
0.88	−0.10233428	−0.228213778	−0.378651772
0.9	−0.146585872	−0.317988588	−0.519668905
0.92	−0.201030173	−0.419825542	−0.678129639
0.94	−0.264804016	−0.535847227	−0.842021671
0.96	−0.338272374	−0.667851621	−1.027004629
0.98	−0.435525245	−0.811083227	−1.2305268
1	−0.553159942	−0.990804058	−1.460123343

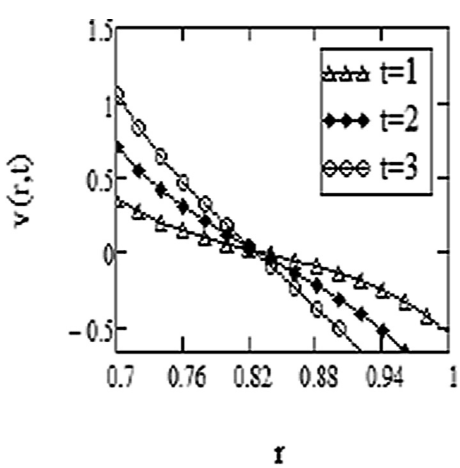

Fig. 2 $\tau(r,t)$, Eq. (26) for $R_1=0.5$, $R_2=1$, $\Omega_1=1$, $\Omega_1=-1$, $\lambda=6$, $\lambda_1=3$, $\lambda_r=1$, $v=5$, $\alpha=0.01$, $\beta=1$, $\mu=2.196$ and distinctness in time.

Finally,

$$\bar{\tau}(r,q)=\kappa\left[\left[\frac{X(q)}{I_1(R_1D)}-\frac{K_1(R_1D)}{K_1(R_2D)I_1(R_1D)-K_1(R_1D)I_1(R_2D)}\times\left(Y(q)-X(q)\frac{I_1(R_2D)}{I_1(R_1D)}\right)\right]\left[DI_0(rD)-2\frac{I_1(rD)}{r}\right]-\left[\frac{I_1(R_1D)}{K_1(R_2D)I_1(R_1D)-K_1(R_1D)I_1(R_2D)}\times\left(Y(q)-X(q)\frac{I_1(R_2D)}{I_1(R_1D)}\right)\right]\left[DK_0(rD)+2\frac{K_1(rD)}{r}\right]\right].$$

Table 2 $v_\theta(r,t)$, Eq. (22) for $R_1=0.7$, $R_2=1$, $\Omega_1=0.5$, $\Omega_1=-0.5$, $\lambda_1=1.5$, $\lambda_r=0.9$, $v=0.005, \alpha=0.01$, $\beta=1$, t = 2, distinctness in λ.

r	$v_\theta(r,t)$ $\lambda=1$	$v_\theta(r,t)$ $\lambda=3$	$v_\theta(r,t)$ $\lambda=5$
0.7	0.700001901	0.700002503	0.6999999
0.72	0.475716367	0.434778386	0.402504106
0.74	0.319242771	0.266721472	0.228119409
0.76	0.209937291	0.161068771	0.127345027
0.78	0.13266965	0.094589625	0.069519477
0.8	0.076263419	0.051895585	0.036026897
0.82	0.032256981	0.022664539	0.015556796
0.84	−0.006074908	−0.00041152	0.000927775
0.86	−0.044625237	−0.023169721	−0.013087258
0.88	−0.0891884	−0.051270661	−0.031414038
0.9	−0.146228758	−0.091427519	−0.060205296
0.92	−0.223636718	−0.152773987	−0.108631526
0.94	−0.331637788	−0.248590367	−0.191283252
0.96	−0.483768084	−0.398549671	−0.331576058
0.98	−0.698139885	−0.631567555	−0.56640165
1	−0.998739023	−0.989493336	−0.951957794

Table 3 $v_\theta(r,t)$, Eq. (22) for $R_1=0.7$, $R_2=1$, $\Omega_1=0.5$, $\Omega_1=-0.5$, $\lambda=1$, $\lambda_r=1$, $v=0.005, \alpha=0.02$, $\beta=1$, t = 2.5, distinctness in λ_1.

r	$v_\theta(r,t)$ $\lambda_1=1$	$v_\theta(r,t)$ $\lambda_1=3$	$v_\theta(r,t)$ $\lambda_1=6$
0.7	0.875000554	0.875004062	0.875001219
0.72	0.626891366	0.577549592	0.520671831
0.74	0.442154385	0.376075913	0.304842052
0.76	0.303839367	0.240223874	0.175402689
0.78	0.198514818	0.148128931	0.098391503
0.8	0.115441362	0.084016634	0.052089561
0.82	0.04590786	0.036347901	0.022669981
0.84	−0.017544043	−0.003769364	0.000917166
0.86	−0.081703587	−0.043914445	−0.020151485
0.88	−0.153302761	−0.091545603	−0.04719358
0.9	−0.23954511	−0.155153059	−0.088341755
0.92	−0.348714813	−0.245495471	−0.155222897
0.94	−0.490742042	−0.376987399	−0.265521831
0.96	−0.677874203	−0.569381503	−0.446281105
0.98	−0.92515459	−0.849748714	−0.737926281
1	−1.251324279	−1.254375587	−1.19813967

4. Numerical results

By using Gaver-Stehfest algorithm Eq. (3) [28] some numerical results are obtained against different physical parameters,

4.1. Special case

Invoke $\lambda_1\to 0$ in Eqs. (17) and (23) the calculated numerical results reduced to fractional Oldroyd-B fluid. Some numerical results for fractional Oldroyd-B fluid are in Tables 13 and 14. These results are exactly same as already calculated results by Wang et al. [25].

5. Results and discussion

In this article solution for fractional Burgers' fluid in annulus is determined by semi analytical technique in which integral transform and modified bessel equation is used. Some numer-

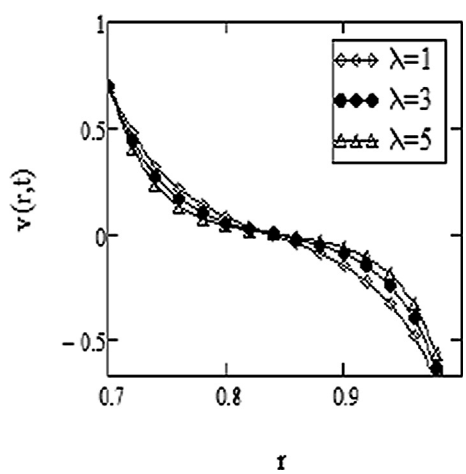

Fig. 3 $v_\theta(r,t)$, Eq. (22) for $R_1=0.7, R_2=1, \Omega_1=0.5, \Omega_1=-0.5$, $\lambda_1=1.5, \lambda_r=0.9, v=0.005, \alpha=0.01, \beta=1$, t = 2 and distinctness in λ.

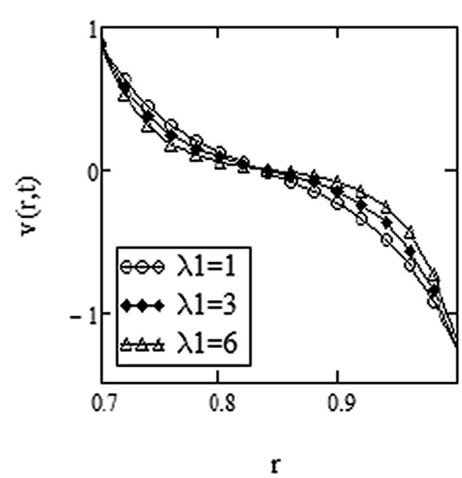

Fig. 4 $v_\theta(r,t)$, Eq. (22) for $R_1=0.7, R_2=1, \Omega_1=0.5, \Omega_1=-0.5$, $\lambda=1$, $\lambda_r=1$, $v=0.005, \alpha=0.02, \beta=1$, t = 2.5 and distinctness in λ_1.

ical techniques are used for final expression i.e. Stehfest's algorithm Eq. (3) [28]. In the end there are some graphs to discuss the reaction of physical parameters on calculated result. To check the legitimacy of the arrangement there are comparisons with another algorithm named, Tzou's algorithm for velocity and shear stress Eq. (4) [29]. By applying some limits the result is reduced to fractional Oldroyd-B fluid, these results are exactly same as already calculated results by Wang et al. [25] (see Fig. 1).

Table 1 and Fig. 2 are for the effect of time on velocity field, by increase in time velocity increases and near the inner cylinder velocity is zero this argument is also theocratically true because inner cylinder radius is less than the outer cylinder. Table 2, 3 and Figs. 3, 4 are for effect of relaxation times 'λ' and 'λ_1' on velocity field. Clearly when the value of relaxation time increase the velocity field is gradually decreases. Table 4 and Fig. 5 are for influence of retardation time 'λ_r', by increase in 'λ_r' velocity function is also increases. Since behavior of relaxation time and retardation time are opposite in direction therefore our solution satisfied the theocratical results. Table 5 and Fig. 6 demonstrates the effect of Kinematic viscosity ν, velocity is increasing function of ν. Table 6 and Fig. 7 are for the effect of time on shear stress, by increase in time stress increases. Table 7, 8 and Figs. 8, 9 are for effect of relaxation times 'λ' and 'λ_1' on shear stress. Clearly when the value of relaxation time increase the stress is gradually decreases. So, stress is decreasing function of relaxation time. Table 9 and Fig. 10 are for influence of retardation time 'λ_r', by increase in 'λ_r' stress is also increases. Since behavior of relaxation time and retardation time are opposite in direction therefore our solution satisfied the theocratical results. Table 10 and Fig. 11 shows the effect of dynamic viscosity μ, stress is

Table 4 $v_\theta(r,t)$, Eq. (22) for $R_1 = 0.7, R_2 = 1, \Omega_1 = 0.5, \Omega_1 = -0.5, \lambda = 6, \lambda_1 = 6, t = 2, \nu = 0.009, \alpha = 0.01, \beta = 0.8$, distinctness in λ_r.

r	$v_\theta(r,t)$ $\lambda_r = 1$	$v_\theta(r,t)$ $\lambda_r = 3$	$v_\theta(r,t)$ $\lambda_r = 6$
0.7	0.699998929	0.699999647	0.700004858
0.72	0.418237345	0.476737997	0.513301258
0.74	0.245491367	0.321310837	0.370431333
0.76	0.141382907	0.212415027	0.259521199
0.78	0.079263808	0.134847466	0.171321359
0.8	0.041938236	0.077564455	0.098492568
0.82	0.018323731	0.032309623	0.034998685
0.84	0.000982602	−0.007486767	−0.024347638
0.86	−0.015733342	−0.04755925	−0.084310131
0.88	−0.037178772	−0.093543962	−0.149575378
0.9	−0.06980599	−0.151720877	−0.225106608
0.92	−0.122636538	−0.229785487	−0.316541523
0.94	−0.20901483	−0.33776056	−0.430508031
0.96	−0.348441022	−0.489053993	−0.575110963
0.98	−0.568316742	−0.702054771	−0.760524618
1	−0.90384878	−1.001863725	−0.999558035

Table 5 $v_\theta(r,t)$, Eq. (22) for $R_1 = 0.7, R_2 = 1, \Omega_1 = 0.5, \Omega_1 = -0.5, \lambda = 2, \lambda = 3, \lambda_r = 0.5, t = 1, \alpha = 0.01, \beta = 0.9$, distinctness in ν.

r	$v_\theta(r,t)$ $\nu = 0.01$	$v_\theta(r,t)$ $\nu = 0.015$	$v_\theta(r,t)$ $\nu = 0.03$
0.7	0.350001437	0.350002593	0.350000487
0.72	0.20707432	0.227196272	0.254084329
0.74	0.120553348	0.145501475	0.181452395
0.76	0.068987343	0.091488484	0.126026081
0.78	0.038491706	0.055661853	0.082946071
0.8	0.020287352	0.031318826	0.048262269
0.82	0.008810512	0.013674882	0.018703539
0.84	0.000379947	−0.000876118	−0.008563741
0.86	−0.007784148	−0.0153553	−0.036151506
0.88	−0.018334884	−0.032713859	−0.066642294
0.9	−0.034534742	−0.056328704	−0.102775877
0.92	−0.061097743	−0.090540297	−0.147648314
0.94	−0.105248575	−0.141245182	−0.204900384
0.96	−0.178157417	−0.216629137	−0.278910911
0.98	−0.296746268	−0.327974668	−0.375044446
1	−0.485660607	−0.490478767	−0.49977694

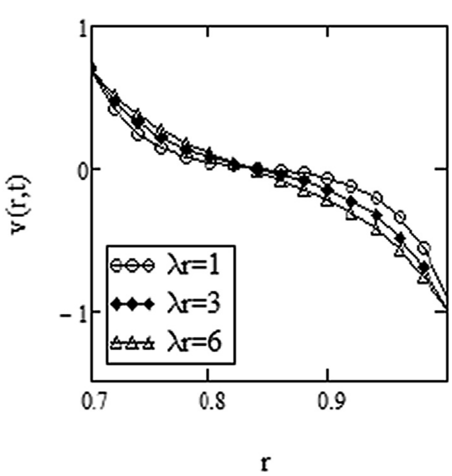

Fig. 5 $v_\theta(r,t)$, Eq. (22) for $R_1 = 0.7, R_2 = 1, \Omega_1 = 0.5, \Omega_1 = -0.5, \lambda = 6, \lambda_1 = 6, t = 2, \nu = 0.009, \alpha = 0.01, \beta = 0.8$ and distinctness in λ_r.

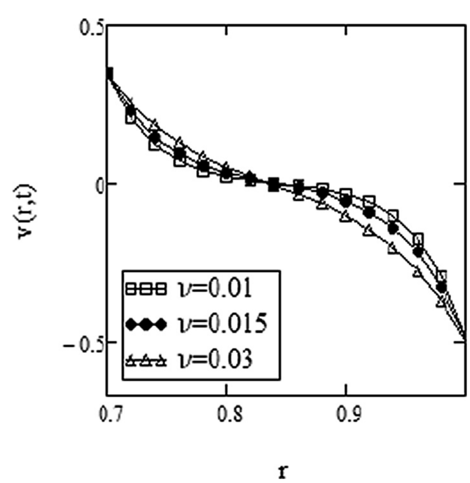

Fig. 6 $v_\theta(r,t)$, Eq. (22) for $R_1 = 0.7, R_2 = 1, \Omega_1 = 0.5, \Omega_1 = -0.5, \lambda = 2, \lambda = 3, \lambda_r = 0.5, t = 1, \alpha = 0.01, \beta = 0.9$ and distinctness in ν.

Table 6 $\tau(r,t)$, Eq. (26) for $R_1 = 0.5, R_2 = 1, \Omega_1 = 1, \Omega_1 = -1, \lambda = 6, \lambda_1 = 3, \lambda_r = 1, \nu = 5, \alpha = 0.01, \beta = 1, \mu = 2.196$, distinctness in time.

r	$\tau(r,t)$ t = 0.6	$\tau(r,t)$ t = 0.7	$\tau(r,t)$ t = 0.8
0.5	−1.377689922	−1.616312078	−1.844534396
0.53	−1.216719232	−1.428627952	−1.639561387
0.56	−1.085959294	−1.283239312	−1.460814594
0.59	−0.975932771	−1.147551621	−1.317187027
0.62	−0.882680329	−1.03840408	−1.187063406
0.65	−0.801474454	−0.944387669	−1.083755976
0.68	−0.737906551	−0.867213055	−0.988454733
0.71	−0.680445113	−0.797338174	−0.910204725
0.74	−0.627301346	−0.739834595	−0.8405767
0.77	−0.581742975	−0.683762868	−0.783185291
0.8	−0.545115071	−0.640682282	−0.72965888
0.83	−0.512274632	−0.600927419	−0.68537686
0.86	−0.483776928	−0.568288734	−0.64754883
0.89	−0.460002607	−0.536438453	−0.615450542
0.92	−0.439665401	−0.513959783	−0.582323103
0.95	−0.422604044	−0.492829038	−0.563150871
0.98	−0.40649706	−0.474286133	−0.542630537

Table 7 $\tau(r,t)$, Eq. (26) for $R_1 = 0.5, R_2 = 1, \Omega_1 = 1, \Omega_1 = -1, t = 1, \lambda_1 = 2, \lambda_r = 2, \nu = 1, \alpha = 0.1, \beta = 0.1, \mu = 2.196$, distinctness in λ.

r	$\tau(r,t)$ $\lambda = 5$	$\tau(r,t)$ $\lambda = 6$	$\tau(r,t)$ $\lambda = 7$
0.5	−2.837707444	−2.517215716	−2.260829341
0.53	−2.506395207	−2.222328583	−1.985660931
0.56	−2.234506531	−1.976965655	−1.773518732
0.59	−2.001496726	−1.775103236	−1.584780039
0.62	−1.808011955	−1.600640457	−1.432822914
0.65	−1.645551619	−1.4582054	−1.300188882
0.68	−1.505961663	−1.336093915	−1.193572097
0.71	−1.391936474	−1.236574845	−1.100153569
0.74	−1.293666764	−1.149584073	−1.025636393
0.77	−1.21015949	−1.078366792	−0.961813469
0.8	−1.143456593	−1.020606896	−0.908827744
0.83	−1.085540858	−0.97450405	−0.864787168
0.86	−1.040977402	−0.932417003	−0.831773179
0.89	−1.000501135	−0.90049389	−0.806997195
0.92	−0.970301675	−0.88150462	−0.781075964
0.95	−0.944245262	−0.869620833	−0.771469779
0.98	−0.935700702	−0.851220878	−0.75911236

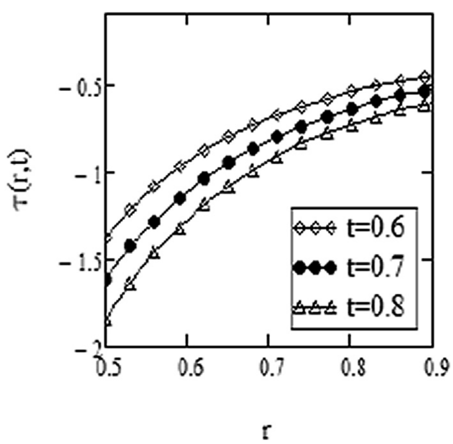

Fig. 7 $\tau(r,t)$, Eq. (22) for $R_1 = 0.7$, $R_2 = 1$, $\Omega_1 = 0.5$, $\Omega_1 = -0.5$, $t = 2$, $\lambda_r = 0.5$, $\nu = 0.005$, $\alpha = 0.02$, $\beta = 0.9$ and distinctness in t.

Table 8 $\tau(r,t)$, Eq. (26) for $R_1 = 0.5, R_2 = 1, \Omega_1 = 1, \Omega_1 = -1, t = 1, \lambda = 4, \lambda_r = 1, \nu = 1, \alpha = 0.1, \beta = 0.1, \mu = 2.196$, distinctness in λ_1.

r	$\tau(r,t)$ $\lambda_1 = 2$	$\tau(r,t)$ $\lambda_1 = 3$	$\tau(r,t)$ $\lambda_1 = 4$
0.5	−3.117232746	−2.696147765	−2.376018946
0.53	−2.739182573	−2.383059978	−2.078583516
0.56	−2.443048394	−2.102108489	−1.853900129
0.59	−2.179029359	−1.880845966	−1.653709141
0.62	−1.969765148	−1.701584557	−1.493208448
0.65	−1.791598415	−1.550973137	−1.357886641
0.68	−1.645864454	−1.421660153	−1.249681219
0.71	−1.519556543	−1.318671302	−1.160319473
0.74	−1.418894706	−1.233754532	−1.087388703
0.77	−1.335315379	−1.16379884	−1.030031956
0.8	−1.264823421	−1.110035075	−0.987346505
0.83	−1.210525373	−1.06430836	−0.954451999
0.86	−1.165247337	−1.036370637	−0.926350339
0.89	−1.135820628	−1.013708648	−0.915566848
0.92	−1.112433812	−1.004004629	−0.909071502
0.95	−1.107621135	−0.993596277	−0.908669261
0.98	−1.089549715	−1.000794966	−0.923161498

increasing function of μ. Table 11, 12 and Figs. 12, 13 and are comparison between values of two numerical algorithms for velocity field and shear stress to check the accuracy. Clearly, results with both algorithms are approximately same.

6. Conclusion

Conclusively, The semi analytical expressions for velocity field and associated shear stress for the rotational flow of fractional Burgers fluid model through two rotating cylinders are obtained, with the help of integral transform and Bessel equation. For the conversion of governing equations into fractional derivative form by usingRiemann-Liouville fractional differential operator. The inverse Laplace transform has been calculated by using MATHCAD. To check the legitimacy of the arrangement there are comparisons with another algorithm named, Tzou's algorithm for velocity and shear stress [29]. The validation of numerical results is also presented. The behavior of physical parameters have been performed graphically. The comparison between numerical and exact results are also presented in tabular and graphical form.

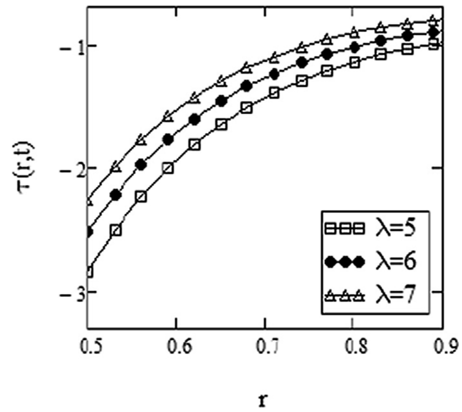

Fig. 8 $\tau(r,t)$, Eq. (26) for $R_1 = 0.5$, $R_2 = 1$, $\Omega_1 = 1$, $\Omega_1 = -1$, $t = 1$, $\lambda_1 = 2$, $\lambda_r = 2$, $v = 1, \alpha = 0.1$, $\beta = 0.1$, $\mu = 2.196$ and distinctness in λ.

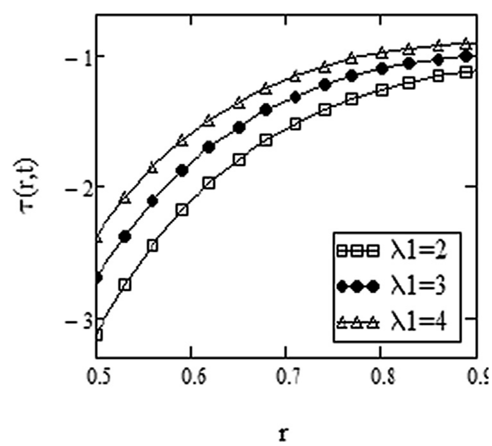

Fig. 9 $\tau(r,t)$, Eq. (26) for $R_1 = 0.5$, $R_2 = 1$, $\Omega_1 = 1$, $\Omega_1 = -1$, $t = 1$, $\lambda = 4$, $\lambda_r = 1$, $v = 1, \alpha = 0.1$, $\beta = 0.1$, $\mu = 2.196$ and distinctness in λ_1.

Table 9 $\tau(r,t)$, Eq. (26) for $R_1 = 0.5$, $R_2 = 1$, $\Omega_1 = 1$, $\Omega_1 = -1$, $\lambda = 6$, $\lambda_1 = 0.5$, $t = 0.8$, $v = 1, \alpha = 0.8$, $\beta = 0.5$, $\mu = 2.196$, distinctness in λ_r.

r	$\tau(r,t)$ $\lambda_r = 3$	$\tau(r,t)$ $\lambda_r = 4$	$\tau(r,t)$ $\lambda_r = 5$
0.5	−1.467093203	−1.681483454	−1.854181503
0.53	−1.281281168	−1.476002066	−1.632398073
0.56	−1.131222385	−1.307647416	−1.450581411
0.59	−1.008537118	−1.168573048	−1.297320809
0.62	−0.909110238	−1.054355764	−1.171155623
0.65	−0.827922748	−0.958995163	−1.066294215
0.68	−0.762889619	−0.880450232	−0.97745611
0.71	−0.711266174	−0.816371255	−0.903992465
0.74	−0.671113903	−0.764086231	−0.842672445
0.77	−0.641141003	−0.722082631	−0.792429062
0.8	−0.620167407	−0.689050113	−0.750851289
0.83	−0.607176068	−0.663809829	−0.717486083
0.86	−0.600079039	−0.645474234	−0.6910437
0.89	−0.601844704	−0.632621254	−0.670726351
0.92	−0.607840874	−0.626727286	−0.654293367
0.95	−0.623571791	−0.625372806	−0.641994779
0.98	−0.640606499	−0.628031826	−0.634192068

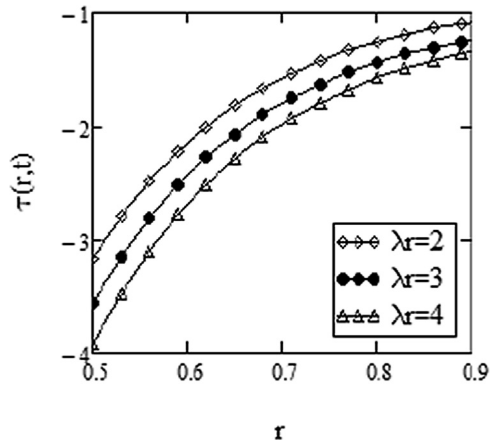

Fig. 10 $\tau(r,t)$, Eq. (26) for $R_1 = 0.5$, $R_2 = 1$, $\Omega_1 = 1$, $\Omega_1 = -1$, $\lambda = 6$, $\lambda_1 = 0.5$, $t = 0.8$, $v = 1, \alpha = 0.8$, $\beta = 0.5$, $\mu = 2.196$ and distinctness in λ_r.

Table 10 $\tau(r,t)$, Eq. (26) for $R_1 = 0.5$, $R_2 = 1$, $\Omega_1 = 1$, $\Omega_1 = -1$, $\lambda = 6$, $\lambda_1 = 2$, $\lambda_r = 1$, $v = 3, \alpha = 0.5$, $\beta = 0.5$, $t = 1$, distinctness in μ.

r	$\tau(r,t)$ $\mu = 2.196$	$\tau(r,t)$ $\mu = 2.496$	$\tau(r,t)$ $\mu = 2.896$
0.5	−1.850647002	−2.102912475	−2.439670001
0.53	−1.637145546	−1.861021229	−2.159021349
0.56	−1.458154169	−1.657100177	−1.922121178
0.59	−1.309352833	−1.48835082	−1.726725268
0.62	−1.182868715	−1.344765559	−1.560232938
0.65	−1.076320636	−1.22343137	−1.419342517
0.68	−0.98612869	−1.12083439	−1.300664663
0.71	−0.909049853	−1.033347262	−1.198570608
0.74	−0.84370423	−0.959045625	−1.112867576
0.77	−0.788222927	−0.895881176	−1.039586209
0.8	−0.740791976	−0.841889023	−0.977153072
0.83	−0.700746789	−0.796748358	−0.924482497
0.86	−0.666431384	−0.757872544	−0.879015445
0.89	−0.639467079	−0.726700327	−0.843316449
0.92	−0.61584704	−0.70028679	−0.812447938
0.95	−0.596528657	−0.678298479	−0.787354408
0.98	−0.5820251	−0.661476997	−0.76784829

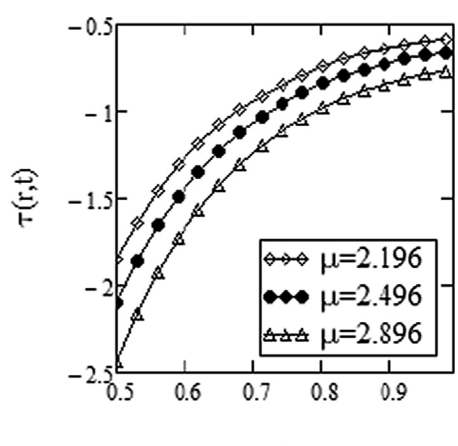

Fig. 11 $\tau(r,t)$, Eq. (26) for $R_1 = 0.5$, $R_2 = 1$, $\Omega_1 = 1$, $\Omega_1 = -1$, $\lambda = 6$, $\lambda_1 = 2$, $\lambda_r = 1$, $v = 3, \alpha = 0.5$, $\beta = 0.5$, $t = 1$ and distinctness in μ.

Table 11 Comparison of velocity field corresponding to Stehfest's Eq. (3) [28], Tzou's algorithm Eq. (4) [29] for $R_1 = 0.7$, $R_2 = 1$, $\Omega_1 = 0.81$, $\Omega_1 = -0.4$, $\lambda = 2$, $\lambda_1 = 3$, $\lambda_r = 1$, $\nu = 2$, $\alpha = 0.01$, $\beta = 0.62$, $t = 0.65$.

r	$v_\theta(r,t)$ Stehfest's [28]	$v_\theta(r,t)$ Tzou's [29]	Difference
0.7	0.3185168	0.317502391	−0.001014
0.72	0.2689977	0.270848126	0.0018504
0.74	0.2259899	0.225927008	−0.0000629
0.76	0.1828824	0.182574432	−0.000308
0.78	0.1413106	0.140640833	−0.00067
0.8	0.0994774	0.099989824	0.0005125
0.82	0.060923	0.060496601	−0.000426
0.84	0.0226571	0.022046573	−0.00061
0.86	−0.015887	−0.015465818	0.0004211
0.88	−0.052486	−0.052138119	0.0003474
0.9	−0.088967	−0.088060757	0.0009063
0.92	−0.123544	−0.123317815	0.0002257
0.94	−0.1581	−0.157987709	0.0001123
0.96	−0.192385	−0.192143787	0.000241
0.98	−0.227296	−0.225854852	0.0014416
1	−0.259805	−0.259185625	0.0006192

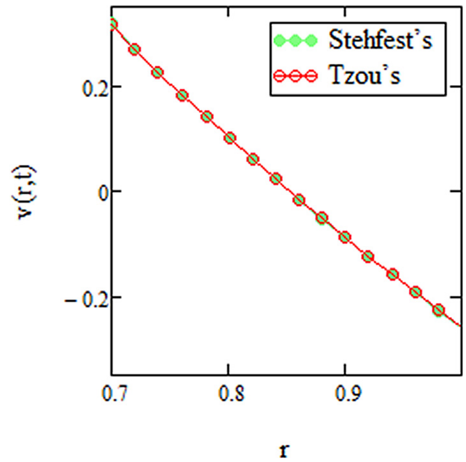

Fig. 12 The velocity area related to Stehfest's [28] and Tzou's algorithm [29] for $R_1 = 0.7$, $R_2 = 1$, $\Omega_1 = 0.81$, $\Omega_1 = -0.4$, $\lambda = 2$, $\lambda_1 = 3$, $\lambda_r = 1$, $\nu = 2$, $\alpha = 0.01$, $\beta = 0.62$, $t = 0.65$.

Table 12 Comparison of Shear stress corresponding to Stehfest's Eq. (3) [28], Tzou's algorithm Eq. (4) [29] for $R_1 = 0.1$, $R_2 = 0.5$, $\Omega_1 = 1.5$, $\Omega_1 = -1$, $\lambda = 9$, $\lambda_1 = 9$, $\lambda_r = 1$, $\nu = 9$, $\alpha = 0.7$, $\beta = 0.59$, $t = 0.8$.

r	$\tau(r,t)$ Stehfest's [28]	$\tau(r,t)$ Tzou's [29]	Diffrence
0.1	−0.345656	−0.346102	0.0004461
0.13	−0.203918	−0.204204	0.0002866
0.16	−0.134526	−0.134654	0.0001277
0.19	−0.095686	−0.095777	0.0000908
0.22	−0.072085	−0.072119	0.00003437
0.25	−0.05688	−0.056886	0.000005721
0.28	−0.046783	−0.046745	−0.0000383
0.31	−0.039908	−0.039878	−0.0000305
0.34	−0.035232	−0.035196	−0.0000362
0.37	−0.032135	−0.032108	−0.0000265
0.4	−0.030162	−0.030164	0.000002739
0.43	−0.029067	−0.029036	−0.000031
0.46	−0.028686	−0.028713	0.00002693
0.49	−0.028687	−0.028802	0.0001144

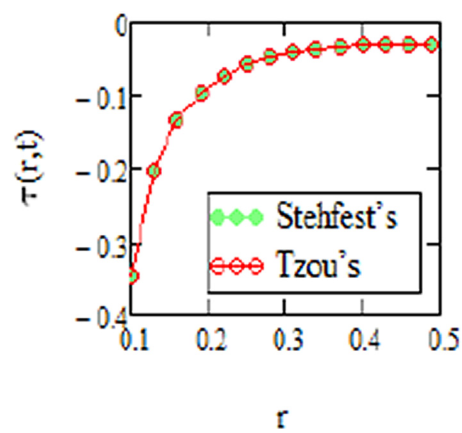

Fig. 13 Comparison of Shear stress corresponding to Stehfest's [28] and Tzou's algorithm [29] for $R_1 = 0.1$, $R_2 = 0.5$, $\Omega_1 = 1.5$, $\Omega_1 = -1$, $\lambda = 9$, $\lambda_1 = 9$, $\lambda_r = 1$, $\nu = 9$, $\alpha = 0.7$, $\beta = 0.59$, $t = 0.8$.

- Velocity is an increasing function of time and retardation time λ_r. It is decreasing function of relaxation times λ, λ_1 and kinematic viscosity.
- Shear stress is an increasing function of time and retardation time λ_r. It is decreasing function of relaxation times λ, λ_1 and dynamic viscosity.
- From the comparison between two numerical algorithms shown in Figs. 12 and 13, numerical values for both algorithms are approximately same for both velocity field and shear stress.

Table 13 $v_\theta(r,t)$, fractional Oldroyd-B fluid [25], for $R_1 = 0.7$, $R_2 = 1, \Omega_1 = 0.5, \Omega_1 = -0.5, \lambda = 2, \lambda_r = 1$, $v = 0.02, \alpha = 0.9, \beta = 0.8$ and distinctness in time.

r	$v_\theta(r,t)$ t = 1	$v_\theta(r,t)$ t = 2	$v_\theta(r,t)$ t = 3
0.7	0.34999747	0.700001573	1.049994245
0.72	0.277363418	0.566118667	0.847364116
0.74	0.214440897	0.442330984	0.656705438
0.76	0.159605368	0.326698184	0.475956796
0.78	0.111171036	0.217326453	0.303243487
0.8	0.067376772	0.11248143	0.136793148
0.82	0.026395122	0.010522165	−0.025043406
0.84	−0.013643711	−0.090086409	−0.183809528
0.86	−0.054632129	−0.190760663	−0.340948741
0.88	−0.098451387	−0.29284024	−0.497819867
0.9	−0.146957353	−0.397572193	−0.655707684
0.92	−0.202009431	−0.506098161	−0.815787029
0.94	−0.265574082	−0.619476896	−0.979256157
0.96	−0.34002255	−0.738766055	−1.147157932
0.98	−0.428675658	−0.864793555	−1.320479664
1	−0.537166236	−0.998480005	−1.500309614

Table 14 $\tau(r,t)$, fractional Oldroyd-B fluid [25], for $R_1 = 0.5, R_2 = 1, \Omega_1 = 1, \Omega_1 = -1, \lambda = 6$, $\lambda_r = 3, v = 5, \alpha = 0.01, \beta = 1, \mu = 2.196$ and distinctness in time.

r	$\tau(r,t)$ t = 0.6	$\tau(r,t)$ t = 0.7	$\tau(r,t)$ t = 0.8
0.5	−3.981149495	−4.655110841	−5.307065097
0.53	−3.549948669	−4.14247502	−4.716717216
0.56	−3.174594974	−3.706268258	−4.218337712
0.59	−2.862880932	−3.330685168	−3.808977538
0.62	−2.582281886	−3.020225522	−3.447943275
0.65	−2.353886006	−2.755798108	−3.141894041
0.68	−2.144383106	−2.505507907	−2.856285714
0.71	−1.972439206	−2.304194385	−2.631234956
0.74	−1.823035005	−2.129817163	−2.424919216
0.77	−1.692170127	−1.969096958	−2.240967586
0.8	−1.560580589	−1.833441375	−2.086103221
0.83	−1.460680046	−1.709819964	−1.946384033
0.86	−1.360597993	−1.58453699	−1.81430395
0.89	−1.272594733	−1.497254181	−1.71026876
0.92	−1.209093623	−1.402404627	−1.594003979
0.95	−1.140952862	−1.330383502	−1.507282993
0.98	−1.069022708	−1.260486902	−1.429302563

Declaration of Competing Interest

The authors declare that they have no known competing financial interests or personal relationships that could have appeared to influence the work reported in this paper.

References

[1] T.W. Ting, Certain non-steady flows of second-order fluids, Arch. Ration. Mech. Anal. 14 (1) (1963) 1–26.
[2] N.D. Waters, M.J. King, The unsteady flow of an elastico-viscous liquid in a straight pipe of circular cross section, J. Phys. D: Appl. Phys. 4 (2) (1971) 204.
[3] C. Fetecău, C. Fetecău, On the uniqueness of some helical flows of a second grade fluid, Acta Mech. 57 (3–4) (1985) 247–252.
[4] K.D. Rahaman, H. Ramkissoon, Unsteady axial viscoelastic pipe flows, J. Non-Newton. Fluid Mech. 57 (1) (1995) 27–38.
[5] W.P. Wood, Transient viscoelastic helical flows in pipes of circular and annular cross-section, J. Non-Newton. Fluid Mech. 100 (1–3) (2001) 115–126.
[6] T. Hayat, A.M. Siddiqui, S. Asghar, Some simple flows of an Oldroyd-B fluid, Int. J. Eng. Sci. 39 (2) (2001) 135–147.
[7] C. Fetecau, Analytical solutions for non-Newtonian fluid flows in pipe-like domains, Int. J. Non-linear Mech. 39 (2) (2004) 225–231.
[8] M. Sajid, T. Hayat, S. Asghar, K. Vajravelu, Analytic solution for axisymmetric flow over a nonlinearly stretching sheet, Arch. Appl. Mech. 78 (2) (2008) 127–134.
[9] C. Fetecau, M. Imran, C. Fetecau, I. Burdujan, Helical flow of an Oldroyd-B fluid due to a circular cylinder subject to time-dependent shear stresses, Z. Angew. Math. Phys. 61 (5) (2010) 959–969.
[10] N. Valliammal, C. Ravichandran, Z. Hammouch, H.M. Baskonus, A new investigation on fractional-ordered neutral differential systems with state-dependent delay, Int. J. Nonlinear Sci. Numer. Simul. 20 (7–8) (2019) 803–809.
[11] S. Qureshi, A. Yusuf, Fractional derivatives applied to MSEIR problems: Comparative study with real world data, Eur. Phys. J. Plus 134 (4) (2019) 171.
[12] C. Cattani, A review on harmonic wavelets and their fractional extension, J. Adv. Eng. Comput. 2 (4) (2018) 224–238.
[13] X.J. Yang, M. Abdel-Aty, Cattani Carlo, A new general fractional order derivative with Rabotnov fractional-exponential kernel applied to model the anomalous heat, Therm. Sci. 23 (3A) (2019) 1677–1681.
[14] Y. Zhaosheng, L. Jianzhong, Numerical research on the coherent structure in the viscoelastic second-order mixing layers, Appl. Math. Mech. 19 (8) (1998) 717–723.
[15] M. Jamil, N.A. Khan, Erratum: Helical flows of fractionalized Burgers' fluids[AIP ADVANCES 2, 012167 (2012)], AIP Adv. 3 (2) (2013) 029901.
[16] S. Roderic, Lakes, Viscoelastic Solids (1999).
[17] G. Degré, P. Joseph, P. Tabeling, S. Lerouge, M. Cloitre, A. Ajdari, Rheology of complex fluids by particle image velocimetry in microchannels, Appl. Phys. Lett. 89 (2) (2006) 024104.
[18] D. Craiem, F.J. Rojo, J.M. Atienza, R.L. Armentano, G.V. Guinea, Fractional-order viscoelasticity applied to describe uniaxial stress relaxation of human arteries, Phys. Med. Biol. 53 (17) (2008) 4543.
[19] D. Craiem, R.L. Armentano, A fractional derivative model to describe arterial viscoelasticity, Biorheology 44 (4) (2007) 251–263.
[20] A. Hernández-Jiménez, J. Hernández-Santiago, A. Macias-Garcıa, J. Sánchez-González, Relaxation modulus in PMMA and PTFE fitting by fractional Maxwell model, Polym. Test. 21 (3) (2002) 325–331.
[21] H. Villinger, Solving cylindrical geothermal problems using the Gaver-Stehfest inverse Laplace transform, Geophysics 50 (10) (1985) 1581–1587.
[22] A. Akgül, E. Karatas, D. Baleanu, Numerical solutions of fractional differential equations of Lane-Emden type by an accurate technique, Adv. Differen. Eqs. 2015 (1) (2015) 1–12.
[23] M.S. Hashemi, M. Inc, E. Karatas, A. Akgül, A numerical investigation on burgers equation by mol-gps method, J. Adv. Phys. 6 (3) (2017) 413–417.

[24] N. Raza, Unsteady rotational flow of a second grade fluid with non-integer Caputo time fractional derivative, Punjab Univ. J. Math 49 (2017) 15–25.
[25] B. Wang, M. Tahir, M. Imran, M. Javaid, C.Y. Jung, Semi analytical solutions for fractional Oldroyd-B fluid through rotating annulus, IEEE Access 7 (2019) 72482–72491.
[26] S. Qureshi, A. Yusuf, S. Aziz, On the use of Mohand integral transform for solving fractional-order classical Caputo differential equations, 2020.
[27] L. Debnath, D. Bhatta, Integral Transforms and their Applications, second ed., Chapman and Hall/CRC Press, Boca-Raton-London-New York, 2006.
[28] A. Kuznetsov, On the Convergence of the Gaver-Stehfest Algorithm, SIAM J. Numer. Anal. 51 (6) (2013) 2984–2998.
[29] D.Y. Tzou, Macro- to Micro-scale Heat Transfer: The Lagging Behavior, Taylor & Francis, Washington, DC, 1997.
[30] M. Khan, S.H. Ali, C. Fetecau, Exact solutions of accelerated flows for a Burgers' fluid, The case $\gamma < \lambda_2/4$, Appl. Math. Comput. 203 (2) (2008) 881–894.
[31] C. Fetecau, T. Hayat, M. Khan, C. Fetecau, A note on longitudinal oscillations of a generalized Burgers fluid in cylindrical domains, J. Non-Newton. Fluid Mech. 165 (7–8) (2010) 350–361.
[32] S.H.A.M. Shah, Some helical flows of a Burgers' fluid with fractional derivative, Meccanica 45 (2) (2010) 143–151.
[33] M. Khan, S.H. Ali, H. Qi, On accelerated flows of a viscoelastic fluid with the fractional Burgers' model, Nonlinear Anal. Real World Appl. 10 (4) (2009) 2286–2296.
[34] M. Khan, A. Anjum, C. Fetecau, H. Qi, Exact solutions for some oscillating motions of a fractional Burgers' fluid, Math. Comput. Model. 51 (5–6) (2010) 682–692.
[35] I. Podlubny, Fractional differential equations, Mathematics in Science and Engineering, vol. 198, 1999.
[36] C.F. Lorenzo, T.T. Hartley, Generalized functions for the fractional calculus, 1999.
[37] N.W. McLachlan, Bessel Functions for Engineers, second ed., Oxford University Press, London, 1955.
[38] Y.L. Luke, Integrals of Bessel functions, McGraw-Hill Book Co., Inc., New York, New York, 1962.